Test of Beam Feedback-free Acceleration at TARN-II

Shin-ichi WATANABE†, Tamaki WATANABE‡, Yoshitsugu ARAKAKI‡, Katsuhisa CHIDA‡,
Masao TAKANAKA* and Mitsutaka KANAZAWA**.

INS, Univ. of Tokyo, Midori-cho 3-2-1, Tanashi-shi, Tokyo, 188 Japan
*RIKEN, Hirosawa 2-1, Wako-shi, Saitama, 351-01 Japan
**NIRS, Anagawa 4-9-1, Inage-ku, Chiba, 263 Japan

ABSTRACT

The synchrotron acceleration system of the TARN-II is being upgraded to accelerate a beam that can be captured the beam without a $\Delta\phi$ and ΔR feedback. The precise control of acceleration frequency F_{rf} is a part of upgrade program. The voltage controlled oscillator (VCO) with a beam feed back loop was replaced by the direct digital synthesizer (DDS). To make sure the acceleration with DDS, B-F_{rf} conversion instrument was improved. A ripple field of the dipole magnet was improved to make sure the generation of accurate B-dot signal. An accuracy of calculated frequency F_{rf} depends on the ring parameters. The circumference and radius of curvature of the ring were calibrated with the calibrated injection beam energy. The betatron tune values were chosen at stable operation point. The 26 MeV Alpha beam was accelerated up to 100 MeV without the beam feedback system.

1 INTRODUCTION

A synchrotron acceleration system comprises a beam feedback system to hold the bunched beam in the moving rf bucket. The beam feedback system is responsible for both $\Delta\phi$ and ΔR controls with the aid of beam-pick up instruments. A signal to noise ratio of the beam instrument become the problems whenever the detectable beam current is lower than the threshold level. So, the beam feedback-free technique aiming at an acceleration of faint beam is needed when the beam instrument is poor.

The beam feedback-free acceleration has been studied after the rf stacking experiment at TARN-II.[1] This technique is available to accelerate a heavy ion beam such as the injected beam from the INS-SF cyclotron. The same technique is also available to accelerate a molecule beam from the same cyclotron. To accelerate the faint beam, present rf acceleration system of TARN-II was reviewed because the rf system was developed based on the beam feedback technique.[2]

The acceleration system of TARN-II has been improved aiming at the beam feedback-free acceleration. The rf signal source, magnet power supply and low level rf control system were improved to accelerate the beam without the beam feedback system. The paper describes the improved instruments and beam acceleration test at TARN-II. The Fig.1 shows block diagram of the rf acceleration system and related beam monitor system.

2 DIRECT DIGITAL SYNTHESIZER

An original rf signal generator was a voltage controlled oscillator (VCO) with a phase lock loop. The VCO was replaced by the DDS (direct digital synthesizer) that is responsible for generation of precise continuous sine wave. The DDS is also superior to make the accurate moving rf bucket since the VCO has a large level of spurious noise around the oscillation frequency.

A previous version of DDS in place of the VCO is being used in the CERN-LEAR, GSI-ESR and NIRS-HIMAC. The application note on DDS is appeared in the literature.[3] The DDS is one of the digital rf components using the advanced LSI technology. We chose a board type DDS with on-board x-tall oscillator. The applied DDS module comprises the AD9955 with a control data length of 32-bit.

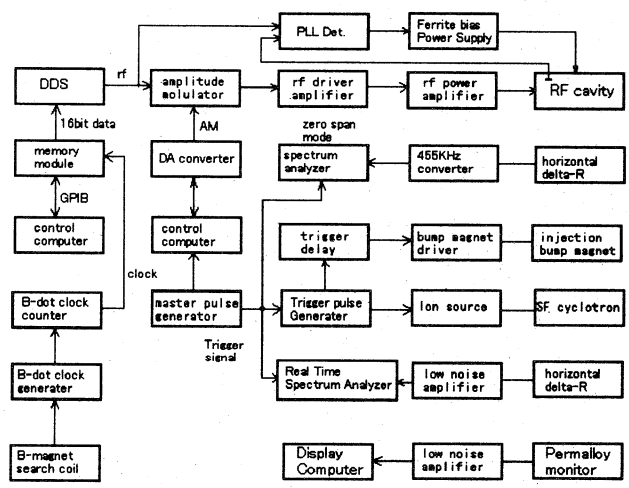

Fig.1 Block diagram of improved rf acceleration system and related beam monitor system.

The control data is responsible for the determination of the oscillation frequency. A control computer generates the rf frequency data. The rf frequency data is calculated based on the following B-F_{rf} equation.

$$F_{rf} = ch/2\pi R/[1+(m_0c^2/300\varepsilon Bp)^2]^{1/2}$$

where ε is charge to mass ratio, q/A.

The rf acceleration voltage, $V\sin\phi_S$, is given by,

$V\sin\phi_S = 2\pi\rho R\,dB/dt$

where dB/dt is B-dot clock rate (Gauss/sec).

A current pattern of the lattice magnet was a trapezoid wave-form. A bottom of the current pattern was subjected to accumulate a beam at the injection energy. A digital memory module (DMM) is subjected to store the data of rf frequency from the capture to the top of the synchrotron acceleration. The data length of DMM is 16 bit. So, the frequency resolution is $F_{rf}/2^{16}$ per bit however the inherent frequency resolution of DDS is 2^{32}. The oscillation frequency F_{rfmax} at the full bit data is designed at 5.368709 MHz. So, the frequency step corresponds 81.921Hz/bit. The spurious noise and 2nd harmonics around the oscillation frequency 1MHz are -67 dB and -46 dB, respectively. The measurement result shows that the phase jump due to a change of control data of DDS is smoothly continued. This means a lack of moving rf bucket is not appeared. The change of oscillation frequency take 5 ns after a data-write command is received.

The B-dot clock signal is subjected to read the frequency data stored in the DMM. The resolution of the B-dot clock signal is responsible for determination of the step-height of frequency data. The B-dot clock generator has a resolution of 1.0, 0.5 and 0.25 Gauss/pulse. Fig. 2 shows an equivalent circuit (upper) of B-dot clock generator and their response (lower) calculated by MATLAB. The lower shows that ramped B signal is converted to the B-dot count number with a time-lag.

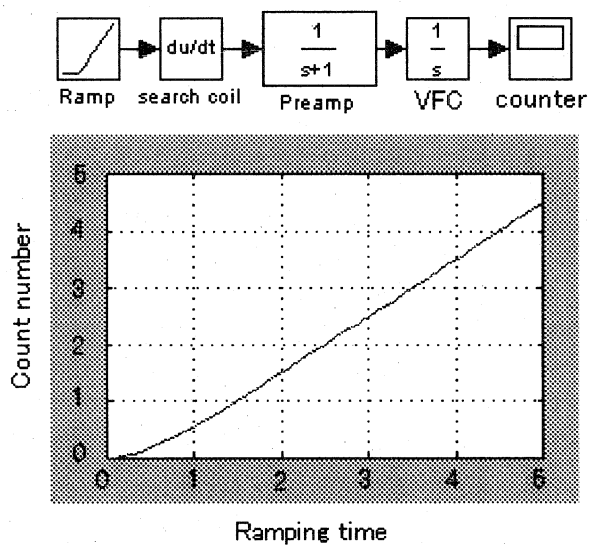

Fig.2 Circuit model and signal response of B-dot clock generator.

A B-dot clock counter accumulates a count number of the B-dot clock signal. When the accumulated count number coincides with a preset number, a reset signal is generated aiming at clear the DMM. The preset number means an expected magnetic field at the flat-top of the dipole magnet current. The readout sequence of acceleration frequency data is stopped then. As shown in Fig.2, the delay of the count number result in the error of readout frequency data. So, the error due to this reason should be corrected. The correction of this error was carried out by means of correction of the frequency data of DMM per readout clock.

3 RIPPLE REDUCTION OF DIPOLE MAGNET CURRENT

The B-dot signal was measured by a search coil located in the gap of dipole magnet. The search coil is sensitive to the noise since the dB/dt of the noise is higher than the ramping speed of excitation field. A ripple component in the magnetic field is to be set as low as possible from the view point of accurate frequency control. The power supply of a lattice magnet is responsible for reducing a ripple component of the magnetic field. A lap of turn-on of the 12 phases thyristor rectifier generates a spike noise on the output of the power supply. This spike noise becomes the origin of common mode current in the lattice magnet strings. A common mode filter (CMF) was installed between the power supply and the dipole magnet strings. The magnet coil circuit is a series of passive elements where the inductance, resistance and capacitance are included. The detailed circuit of CMF is as shown in Fig.3. The Fig. 3 shows a common ground which means the earth ground. The common-mode currents are transmitted in the series of magnet coil circuits and are partially terminated with the common ground through the parallel impedance of the lattice magnet. The CMF is subjected to block the common mode current pass through the magnet coil circuit. A Cut-off frequency was chosen at near the twelve times the 50Hz. Damping resistor of the CMF was tuned so as to avoid the self oscillation of the power supply. Finally, the insertion effect of CMF was evaluated with the PSpice.

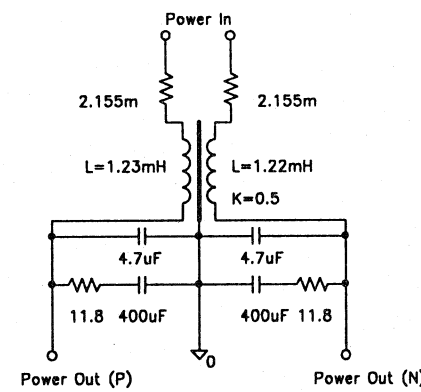

Fig.3 Equivalent circuit of CMF.

The CMF allows the flow of normal excitation current with a small ohmic loss. The CMF acts as a normal mode filter because the mutual coupling constant is 0.5. Due to a limited budged, installed CMF is 1/5 power model of full specifications. The measured specifications of CMF are as follows: Self-inductance = 1.23mH(U) or 1.22mH(D), Ohmic-loss = 2.155 mΩ.

The old DCCT was replaced by the HOLEC-DCCT. The old DCCT has a strong 50Hz noise. The new DCCT is responsible for reducing a 50Hz or higher ripple-currents in the excitation current.

4 BEAM ACCELERATION TEST

An injection energy of Alfa beam was set at 26MeV. A momentum spread and beam current at the exit of SF-cyclotron were set at 0.1% and 0.8 μA, respectively. A transmission efficiency of beam transport line is about 40 % at the injection point of TARN-II.[4] The extracted beam energy from the SF- cyclotron was tuned to match the magnetic rigidity of

TARN-II. The $B\rho$ of extracted beam energy was measured by the analyzer magnet BA-1 where is the one of the beam transport magnets. The slits before and behind the BA-1 were set at 5 mm to center the beam.

The beam orbit of the circulating beam was measured by the ΔR monitor. The Fig.1 shows measurement system. The sum of ΔR signal was down converted to an intermediate frequency 455kHz. The spectrum analyzer was set at zero-span mode to measure the 455kHz. The closed orbit is centered to the mechanical center of ΔR monitor in the ring. A COD of the ring was corrected within +/-0.5 mm.[5]

The average vacuum pressure of the ring was 1×10^{-10} mBar. The betatron tune values of the ring were set at υ_x=1.6088 and υ_y=1.7427, respectively. A life time of the injected beam was 20 seconds. The stored beam current was measured with a beam DCCT. The measured beam intensity was 10μA. It was concluded that a circumference of the ring ($2\pi R$) was 77.712m. The radius of curvature (ρ) of the ring was also concluded at 4.03275±0.00248m. These values were taken into account the calculation of the acceleration frequency, F_{rf}.

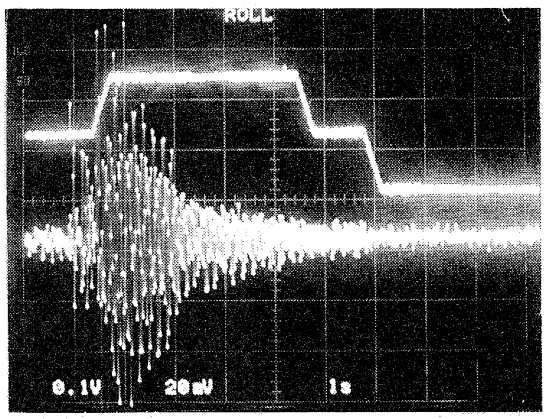

Fig.4 *B*-dot signal and accelerated beam signal.

The acceleration test was carried out after the measurement of property of the injected beam. The *B*-dot clock signal was set at 0.5 Gauss/pulse. In the Fig.4, upper and lower show the *B*-dot signal and the beam intensity, respectively. A rising period of *B*-dot signal comprises the time square process of the magnetic field ramping. The flat top of the magnetic field is identified as a flat region of the *B*-dot signal where the beam signal is disappeared. The top of magnetic field coincides with a beam energy of 100 MeV. From the experiments, we can say that the acceleration efficiency was 12%. The Fig.5 shows accelerated beam intensity and ΔR signal. The upper shows beam position signal from the ΔR monitor. It is recognized that the position of the accelerated beam is slightly moved to the outer side of the vacuum chamber. The following descriptions are brief note on experimental notifications.

First, the beam was captured after the multi-turn beam injection at the flat bottom of the trapezoid magnetic field. As shown in Fig. 1, a phase-lock system of the ferrite bias power supply was tuned so as to track the rf signal from the DDS. The measurement error of *B*-dot signal generator brings the fatal error of acceleration frequency. The fine correction of the acceleration frequency was then required. A real-time spectrum analyzer as shown in Fig.1 was subjected to measure the tracked beam signal or higher harmonics during the beam handling process. The typical operation parameters were as follows: The ramping time of the magnetic field comprises a linear and both the time square regions. The linear region was 3.5 seconds. The time square region near the flat-bottom was 0.3 seconds. The time square region near the flat-top was 0.3 seconds. The injection and top energy fields were set at 1.8152 and 3.5020KG, respectively. The rf frequencies at the injection and top energies of the beam were set at 0.90303 and 1.6963MHz, respectively. The tracking error of ramped excitation current of the lattice magnet family was set within 10^{-3}.

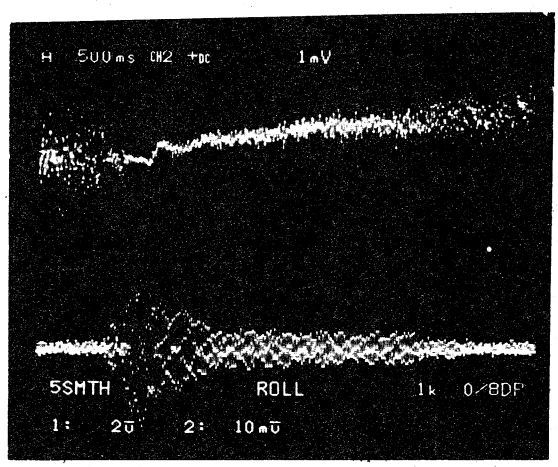

Fig.5 The ΔR (upper) and the intensity (lower) of the accelerated beam.

CONCLUSION

An acceleration efficiency depends on not only the rf bucket-height but also the *B*-dot clock resolution. The rf bucket height was designed to cover the 100% of injected beam. The acceleration efficiency was nearly 12% when the *B*-dot clock resolution was 0.5 Gauss/pulse. It is expected that more precise *B*-dot clock resolution promise the higher acceleration efficiency. The fine tuning of the rf frequency was required at the beginning of acceleration. So, the error of B-F_{rf} converter should be improved since present instrument includes time lag component for the ripple reduction.

ACKNOWLEDGMENT

The first author express his thanks to Prof. Sato, and Mr.Sueno, KEK for their encouragement to improve the power supply. The author also express his thanks to Dr. Goto, RIKEN for his support. The authors thanks Mr. Ono, INS and SF-Cyclotron crew for their operation of SF cyclotron.

REFERENCES

[1] S.Watanabe *et al.* INS-Rep.—1169, Oct. 1996.
[2] T.Katayama *et al.* NI&M in Phys. Res. A 336 (1993) 391-409.
[3] G.C.Schneider PS/RF/Note95-16 , CERN-PS Division.
[4] S.Watanabe *et al.* Proc. of Cyclotrons and Their Applications, Vancouver 1992.
[5] T.Watanabe *et al.* NI&M in Phys. Res. A 381 (1996) 194-208.

† CNS, School of Science, univ. of Tokyo, Tanashi, Tokyo 188.
‡ KEK(Tanashi) , Tanashi, Tokyo 188.